UC San Diego
International Symposium on Stratified Flows

Title

SOMAR-LES for multiscale modeling of internal tide generation

Permalink

https://escholarship.org/uc/item/5w4458tg

Journal

International Symposium on Stratified Flows, 8(1)

Authors

Chalamalla, Vamsi
Santilli, Edward
Scotti, Alberto
et al.

Publication Date

2016-08-29

SOMAR-LES for multiscale modeling of internal tide generation

Vamsi K Chalamalla, Edward Satilli, Alberto Scotti and Sutanu Sarkar

University of North Carolina, Chapel Hill
vchalama@email.unc.edu

Abstract

To represent both large-scale flow and small-scale turbulence, a novel model is developed to study nonlinear processes during the generation and propagation of internal tides. The Stratified Ocean Model with Adaptive Refinement (SOMAR) is used to resolve the large scales, providing the flexibility of block-structured, adaptive mesh refinement along with a suite of numerical tools specifically developed to deal with the high degree of anisotropy of oceanic flows and their attendant numerical challenges. In small, localized regions, we perform a Large Eddy Simulation (LES) to solve the filtered Navier-Stokes Equations and appropriately parametrize the small-scale turbulence. This fine grid LES is driven by the large-scale flow on outer coarse grids which, in turn, receives feedback from the LES in the form of subgrid fluxes. Thus, we are able to efficiently resolve large-scale features of the flow while directing computational power on-the-fly to those small, overturning regions that require small-scale modeling. Simulation of tidal flow past a smoothed triangular bump is performed to demonstrate this new technique. Preliminary analysis show that the new technique is able to assess the most important quantities of the flow such as baroclinic energy conversion and wave flux accurately, and doing so at a much lower computational cost compared to the previous studies.

1   Introduction

Due to the large range of dynamically active scales, ranging from $\mathcal{O}$ (km) down to $\mathcal{O}$ (cm), simulations of oceanic internal tides that resolve the complete range of spatial and temporal scales are well beyond our current capability. Recent studies (Kunze and Toole, 1997; Eriksen, 1998; Laurent et al., 2001; Laurent and Garrett, 2002; Moum et al., 2002; Cacchione et al., 2002; Rudnick et al., 2003; Nash et al., 2004; Aucan et al., 2006) found enhanced turbulence near bottom topographies associated with tidal frequencies. Thus, understanding and quantifying the effect of small scale turbulence and mixing on the large scale flow evolution is important in the context of parameterizing tidal mixing in global circulation models.

The recently developed Stratified Ocean Model with Adaptive Refinement (SOMAR) (Santilli and Scotti, 2011, 2015) has the capability of adaptively refining the grids in localized regions of high non-linearity, allowing it to capture both large-scale and small scale features of the flow at a reduced computational cost. Although the finer grid can resolve energy containing eddies of the flow, expecting it to resolve the smallest scales of the flow will increase the computational cost drastically. Thus, a new model (SOMAR-LES) has been developed, using Large Eddy Simulation on the fine level grid to model the effects of sub-grid scale processes on the resolved scales of the flow. The focus of this paper is to introduce the capabilities of SOMAR-LES by considering a simple internal tide generation problem.

2 Governing equations

In the subsequent discussions of this paper, subscripts C and F represent quantities on the coarse and fine grid respectively.

2.1 Fine grid equations

Filtered Navier-Stokes equations solved on fine level grid are given by

$$\nabla \cdot \overline{\mathbf{u}}_F = 0, \tag{1a}$$

$$\frac{D\overline{\mathbf{u}}_F}{Dt} = -\nabla p_F^* - \overline{b}_F^* \hat{\mathbf{k}} + \nu \nabla^2 \overline{\mathbf{u}}_F - \nabla \cdot \boldsymbol{\tau}, \tag{1b}$$

$$\frac{D\overline{b}_F^*}{Dt} = \kappa \nabla^2 \overline{b}_F^* + \overline{w}_F N^2 - \nabla \cdot \boldsymbol{\lambda}. \tag{1c}$$

Here, $\overline{u}_F, \overline{v}_F, \overline{w}_F$ represent filtered velocities in the streamwise, spanwise, and vertical directions, respectively. Equations (1a)-(1c) will be solved numerically and details of the numerical methods are discussed in the following section. Here, p_F^* denotes the deviation from the background hydrostatic pressure and $\overline{b}_F^*$ denotes the deviation from the background buoyancy stratification. The subgrid scale stress tensor, $\boldsymbol{\tau}$, and the density flux vector, $\boldsymbol{\lambda}$, are given by

$$\tau_{ij} = -2\nu_{sgs}\overline{S}_{ij} \tag{2}$$

and

$$\lambda_j = -\kappa_{sgs}\frac{\partial \overline{b}^*}{\partial x_j}. \tag{3}$$

The LES model is based on the second order filtered structure function (FSF) discussed in Ducros et al. (1996). In this approach, velocity field is filtered using a high-pass Laplacian filter and then computing the structure function from the filtered velocity fields (see Ducros et al. (1996) for details). In the current study, we applied the six-neighbor formulation to calculate the velocity structure function. The sub-grid scale viscosity, ν_{sis}, is given by

$$\nu_{sgs}(\mathbf{x}, t) = 0.0014 C_K^{-3/2} \overline{\Delta} \left(\overline{F_2}(\mathbf{x}, \overline{\Delta}, t) \right)^{1/2} \tag{4}$$

where $\overline{\Delta}$ is the filter width based on the grid size in all directions $(\Delta x\, \Delta y\, \Delta z)^{1/3}$, C_K is the Kolmogorov constant, and $\overline{F_2}$ is the filtered structure function given by

$$\begin{aligned}
\overline{F_2}(\mathbf{x}, t) = \frac{1}{6} \Big(&||\tilde{\overline{u}}_{i+1,j,k} - \tilde{\overline{u}}_{i,j,k}||^2 + ||\tilde{\overline{u}}_{i-1,j,k} - \tilde{\overline{u}}_{i,j,k}||^2 \\
&+ ||\tilde{\overline{u}}_{i,j+1,k} - \tilde{\overline{u}}_{i,j,k}||^2 + ||\tilde{\overline{u}}_{i,j-1,k} - \tilde{\overline{u}}_{i,j,k}||^2 \\
&+ ||\tilde{\overline{u}}_{i,j,k+1} - \tilde{\overline{u}}_{i,j,k}||^2 + ||\tilde{\overline{u}}_{i,j,k-1} - \tilde{\overline{u}}_{i,j,k}||^2 \Big).
\end{aligned}$$

Turbulent Prandtl number of 1 is used to calculate the sub-grid scale diffusivity κ_{sgs}. This model was found to reproduce the energy transfer to the SGS more accurately than the classical Smagorinsky model. For example, Lesieur and Metais (1996) studied boundary layer over a flat plate where the turbulence is temporally and spatially varying. They found that FSF method produces better results when compared to the SF (Metais and Lesieur (1992)) and Smagorinsky methods.

2.2 Coarse grid equations

Navier-Stokes equations solved on coarse level grid are given by

$$\nabla \cdot \mathbf{u}_C = 0, \tag{5a}$$

$$\frac{D\mathbf{u}_C}{Dt} = -\nabla p_C^* - b_C^* \hat{\mathbf{k}} + \nu \nabla^2 \mathbf{u}_C - \nabla \cdot (\boldsymbol{\tau})_{F \rightarrow C}, \tag{5b}$$

$$\frac{Db_C^*}{Dt} = \kappa \nabla^2 b_c^* + w_C N^2 - \nabla \cdot (\boldsymbol{\lambda})_{F \rightarrow C}. \tag{5c}$$

Here, $\boldsymbol{\tau}_{F \rightarrow C}$ and $\boldsymbol{\lambda}_{F \rightarrow C}$ are obtained by averaging $\boldsymbol{\tau}$ and $\boldsymbol{\lambda}$ from the fine grid to the coarse grid.

Synchronization operations are performed when both the coarse and fine level reach the same time. Synchronization involves averaging the velocity and buoyancy fields from the fine to coarse level, repairing fluxes at the coarse-fine interface, and projecting the velocity over the entire heirarchy of grids. The reader is encouraged to refer to Almgren et al. (1998), Martin et al. (2008), and Santilli and Scotti (2015) for details on the synchronization process.

3 Test case results

Table 1: Simulation parameters

parameter	value	comment
U_0	0.15 m/s	barotropic tidal amplitude
Ω	0.1 s^{-1}	tidal forcing frequency
N_{deep}	0.386 s^{-1}	deep ocean stratification
$N_{\text{pyc}}/N_{\text{deep}}$	4	-
h	6.45 m	height of the topography
l	40.0 m	half-width of the obstable
Ex	0.038	low Excursion number
γ	1	steepness parameter

To demonstrate this multi-scale modeling technique, we considered the oscillating tidal flow past smooth triangular bump. The simulation parameters are shown in table 1. The important dimensional parameters for this flow are the barotropic tidal amplitude U_0, length scale of the topography l, height of the topography h, tidal frequency Ω, and background stratification N. The tidal velocity amplitude has been chosen such that the Excursion number is small. The excursion number, Ex, is the important non-dimensional

parameter for this flow, which is defined by the ratio of the distance travelled by a fluid parcel from its mean position (u_0/Ω) to the half-width of the obstacle (l). The steepness parameter, $\gamma = \tan\beta/\tan\alpha$, is the ratio of topographic slope angle, β, to the internal wave characteristic angle, α. The topography has been chosen such that 20% of the ridge is at critical slope. When the slope is near-critical, interaction of the barotropic tide with the sloping topography leads to a resonant response and as a result, strong internal tides are generated from the critical region of the topography. Some fraction of this internal tide energy is dissipated locally due to shear and convective instabilities while the rest of the energy is propagated away from the generation region in the form of low and high mode waves.

Figures 1(a)-(d) show the evolution of fine level grids as the internal tide propagates upward from the generation site. It is important to note that the dynamic grid refinement saves considerable computation time by refining the grid in local regions only when necessary. The grid refinement is done along the beam with a refinement ratio of 4 in the horizontal directions, so that the density overturns near the generation region and non-linear processes associated with the internal tide propagation are well resolved. The vertical grid resolution remains same between the coarse and fine levels.
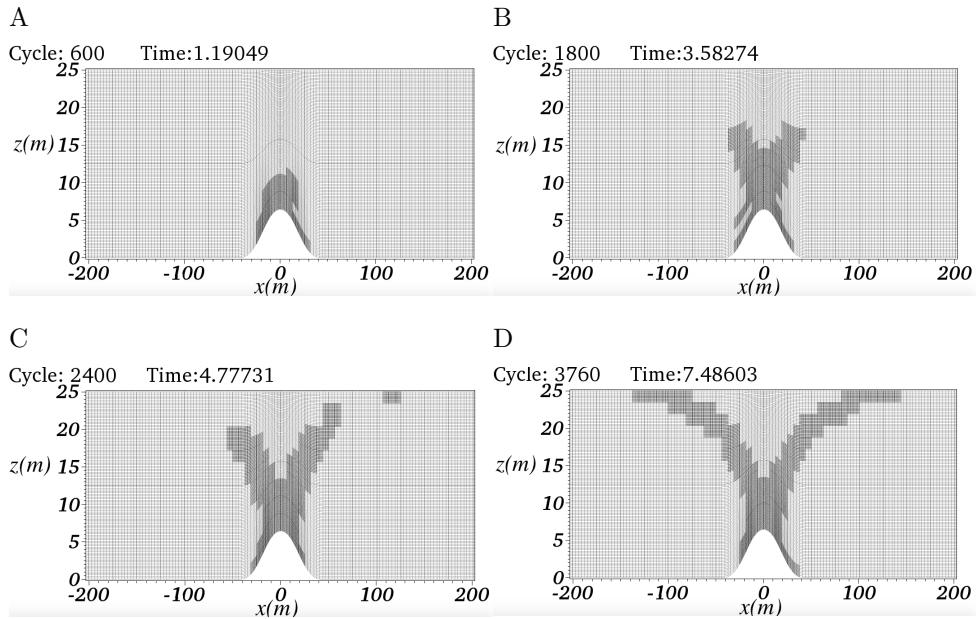

Figure 1: Evolution of the fine-level (LES) grid during the propagation of internal tide towards pycnocline. The grid refinement ratio is 4 in horizontal directions and 1 in the vertical direction.

Figure 2(a) shows stream-wise velocity field at approximately 6.2 tidal cycles. This is the phase at which the barotropic tide has the near-maximum amplitude towards the right in x-direction. As a result, internal tide has its near-maximum velocity amplitude as can be seen in figure 2(a) with strong upward propagating internal tide. The low mode internal wave propagating towards right can be seen at $x \approx +250$ m. Also, there are higher harmonics with frequency 2 and 3 times the tidal frequency propagating upward. They are prominently visible in the vertical velocity field (not shown here) due to the fact that they have strong vertical components owing to the larger angles these harmonics make with the horizontal axis. As the internal tide propagates away from the generation

region, it encounters the pycnocline close to the upper surface. As seen in the figure, interaction of the internal tide with the pycnocline leads to bending of the tidal beam to make a more shallower angle as it propagates upward. Recent studies (Cole et al., 2013; Johnston et al., 2010; Gayen and Sarkar, 2013, 2014) found that when the internal tide interacts with the upper ocean pycnocline, it can lead to strong non-linear phenomenon due to the reduction of vertical length scales and increased shear.
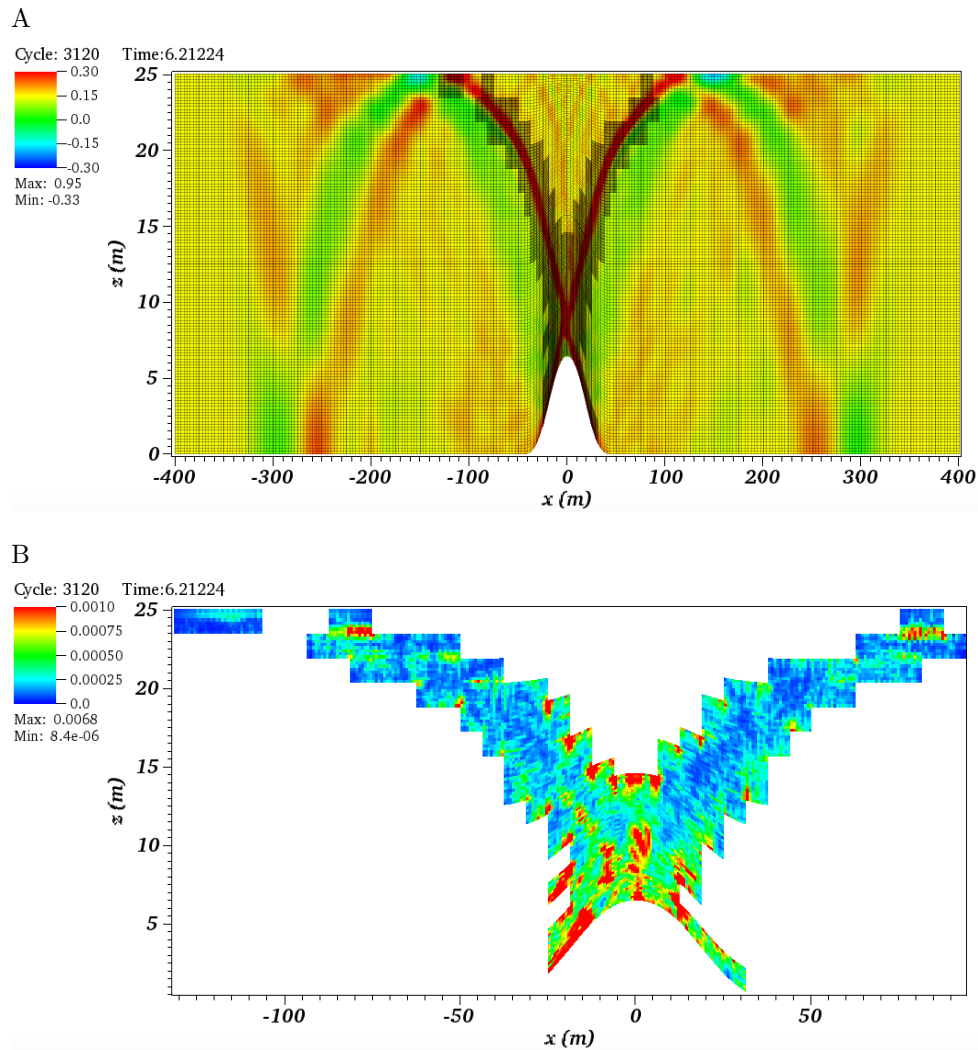

Figure 2: Stream-wise (x-direction)velocity field and sub-grid scale viscosity at $t \approx 6.2T$, where T is tidal period given by $2\pi/\Omega$. Grids on the coarse and fine level are also shown.

Figure 2(b) shows snapshots of the sub-grid viscosity on the fine (LES) level calculated from the filtered structure function shown above. Near the generation region, the sub-grid scale viscosity is elevated by a couple of orders of magnitude due to the presence of small-scale shear and density overturns. As the internal tide moves away from the generation region, the sub-grid scale viscosity gradually decreases. However, the sub-grid scale viscosity is elevated again near the upper surface where the internal tide interacts the pycnocline.

4   Discussion

A new model is used to study the flow near a smoothed triangular bump when the oscillating barotropic tide interacts with the critical region of the topography. With the capability of adaptive, multi-level grids and the large eddy simulation, it is able to resolve important physical phenomena of the flow such as internal tide generation, interaction with the pycnocline, and density overturns near the generation region. Comparison of the SOMAR-LES simulation results with the fully resolved scaled-down DNS simulations (not discussed here) show that SOMAR-LES is able to assess the baroclinic energy conversion and wave flux with a good agreement, and at a much lower computational cost. More detailed quantitative comparisons of the baroclinic energy budget and computational costs will be the object of a forthcoming publication (Chalamalla et al., 2016)

References

Almgren, A. S., Bell, J. B., Colella, P., Howell, L. H., and Welcome, M. L. (1998). A conservative adaptive projection method for the variable density incompressible navier-stokes equations. *Journal of Computational Physics*, 142(1):1 – 46.

Aucan, J., Merrifield, M. A., Luther, D. S., and Flament, P. (2006). Tidal mixing events on the deep flanks of Kaena Ridge, Hawaii. *J. Phys. Oceanogr.*, 36:1202–1219.

Cacchione, D. A., Pratson, L. F., and Ogston, A. S. (2002). The shaping of continental slopes by internal tides. *Science*, 296:724 – 727.

Chalamalla, V., Santilli, E., Scotti, A., and Sarkar, S. (2016). Somar-les: a new modeling framework to bridge the hydrostatic and turbulent scales. *Ocean. Mod.*, In preparation.

Cole, S. T., Rudnick, D. L., Hodges, B. A. ., and Martin, J. P. (2013). Observations of tidal internal wave beams at Kauai Channel, Hawaii. *J. Phys. Oceanogr.*, 39:421–436.

Ducros, F., Comte, P., and Lesieur, M. (1996). Large-eddy simulation of transition to turbulence in a boundary layer developing spatially over a flat plate. *J. Fluid Mech.*, 326:1–36.

Eriksen, C. C. (1998). Internal wave reflection and mixing at Fieberling Guyot. *J. Geophys. Res.*, 103:2977–2994.

Gayen, B. and Sarkar, S. (2013). Degradation of an internal wave beam by parametric subharmonic instability in an upper ocean pycnocline. *J. Geophys. Res.*, 118:4689–4698.

Gayen, B. and Sarkar, S. (2014). Psi to turbulence during internal wave beam refraction through the upper ocean pycnocline. *Geophys. Res. Lett.*, 41:8953–8960.

Johnston, T. M. S., Rudnick, D. L., Carter, G. S., Todd, R. E., and Cole, S. T. (2010). Internal tidal beams and mixing near Monterey Bay. *J. Geophys. Res.*, 116:C03017.

Kunze, E. and Toole, J. M. (1997). Tidally driven vorticity, diurnal shear and turbulence atop Fieberling Seamount. *J. Phys. Oceanogr.*, 27:2663 – 2693.

Laurent, L. C. S. and Garrett, C. (2002). The role of internal tides in mixing the deep ocean. *J. Phys. Oceanogr.*, 32:2882–2899.

Laurent, L. C. S., Toole, J. M., and Schmitt, R. W. (2001). Buoyancy forcing by turbulence above rough topography in the abyssal Brazil Basin. *J. Phys. Oceanogr.*, 31:3476–3495.

Lesieur, M. and Metais, O. (1996). New trends in large-eddy simulations of turbulence. *Annual Review of Fluid Mechanics*, 28:45–82.

Martin, D. F., Colella, P., and Graves, D. (2008). A cell-centered adaptive projection method for the incompressible Navier–Stokes equations in three dimensions. *J. Comput. Phys.*, 227(3):1863–1886.

Metais, O. and Lesieur, M. (1992). Spectral large-eddy simulation of isotropic and stably stratified turbulence. *J. Fluid Mech.*, 239:157– 194.

Moum, J. N., Caldwell, D. R., Nash, J. D., and Gunderson, G. D. (2002). Observations of boundary mixing over the continental slope. *J. Phys. Oceanogr.*, 32:2113–2130.

Nash, J. D., Kunze, E., Toole, J. M., and Schmitt, R. W. (2004). Internal tide reflection and turbulent mixing on the continental slope. *J. Phys. Oceanogr.*, 34:1117–1134.

Rudnick, D. L., Boyd, T. J., Brainard, R. E., Carter, G. S., Egbert, G. D., Gregg, M. C., Holloway, P. E., Klymak, J. M., Kunze, E., Lee, C. M., Levine, M. D., Luther, D. S., Martin, J. P., Merrifield, M. A., Moum, J. N., Nash, J. D., Pinkel, R., Rainville, L., and Sanford, T. B. (2003). From tides to mixing along the hawaiian ridge. *Science*, 301:355 – 357.

Santilli, E. and Scotti, A. (2011). An efficient method for solving elliptic equations on highly anisotropic grids. *J. Comp. Phys.*, 230(23):8342–8359.

Santilli, E. and Scotti, A. (2015). The stratified ocean model with adaptive refinement (somar). *J. Comp. Phys.*, 291:60–81.